FLUIDIZED BED MODEL APPLIED TO FAST PYROLYSIS STUDIES

Davi Hoffmann, davih1@yahoo.com.br
Thamy Cristina Hayashi, thamy@ufba.br
Programa de Pós-graduação em Engª Química - Escola Politécnica – UFBa
Rua Aristides Novis, nº 2 - 2º Andar - Federação, CEP: 40.210-630 Salvador – Bahia

Abstract. *A gas-fluidized bed model in bubbling regime, using a 2D Eulerian approach, including the Kinetic Theory of Granular Flow (KTGF), Geldart B particles and the coefficient drag model of Gidaspow was developed using the framework Fluent 6.3.26, seeking a base model for simulation of a fast pyrolysis reactor in a bubbling fluidized bed. From literature searches were obtained the fluid dynamic models, thebed´s characterization, the dimensions of a bench reactor and strategies to achieve a rapid convergence and stability of the simulation. The convergence is achieved in about seven physical seconds, using as convergence criteria the repetition of the solid volume fraction volume-weighted average profile of the solid velocity and relative pressure at a specific point of the bed. The convergence confirmation is obtained through temporal average solid volume fraction along the bed height. The profile of solid volume fraction shows three distinct behaviors being that the profile obtained in the range between 2.00 and 2.30 seconds is similar to the profile found in the literature, which makes the model suitable for use as basis at future works.*

Keywords*: Fluidized Bed, CFD, Fast Pyrolysis Reactor in Bubbling Fluidized Bed, KTGF, Convergence Criterion*

1. INTRODUCTION

In face of all the environmental problems caused by the use of oil as an energy source, it is important to replace it by renewable sources. Currently ethanol and biodiesel are examples of main substitutes for gasoline and diesel, respectively. However, another source for renewable energy plants is cellulose, which long ago was used as firewood and charcoal.

Unfortunately since cellulose is found in solid state, there is not much flexibility of useif compared to fluids, which limits the possibility of replacing fossil fuels.

One of the ways to turn cellulose into fluid is through fast pyrolysis. In this process, cellulose is thermally degraded in the absence of oxygen, generating gas rich in CO and CO_2 and small fractions of H_2, methane, alkanes, alkenes and alkynes of low molecular weight. Another fluid that may be obtained from cellulose by fat pyrolysis is bio-oil, a dark brown liquid composed of a miscible mixture of water (20-25%) and oxygenated organic compounds (80-75%), and coal. According to Bridgwater and Peacocke (2000), fast pyrolysis yields to bio-oil in the range of 80% when operated close to 500^{o}C and the residence time of products is around one second.

Among the reactors used for this process, we highlight the fluidized bed reactor, consisting of a vertical tubular reactor, which can use nitrogen or treated gas generated in the reaction to fluidize the mixture of organic material and sand. Several works (Bridgwater *et al*, 1999) show that the latter one is used to ensure rapid heat transfer to biomass particles.

The importance of such reactor, according to Depypere *et al* (2004), is due to high rates of heat transfer, supply of gas or heat through the walls, good mix between the solids particles, good controllability and the simple configuration the equipment provides.

Baeyens *et al* (2008) show that the fluid dynamics in the reactor is very important, since the energy and mass transfer, fluidization, temperature and residence time influence the reaction kinetics and hence the yield of products. Since many details of these phenomena are difficult to observe experimentally, the needs of able computational models that can describe such phenomena become important.

Hamzehei and Rahimzade (2009) say that the main difficulty in modeling a fluidized bed is that the interface between two phases are unknown, transient and highly influenced by the size, shape and density of the solid phase particles, which are hardly homogenous, and the velocity of the fluid phase.

According Apte *et al* (2003), one way to model the system taking into account such difficulties would be using the Lagrangian approach, where each particle, with its peculiarities, is considered a discrete element and has a balance of forces associated with each. However, due to the large number of particles present in a fluidized bed, the computational effort becomes an obstacle to the use of such approach.

The Eulerian approach, using the kinetic theory of granular flows, is the most used in these cases because it presents a less computational effort compared to the Lagrangian one, and despite the simplifications, several studies (Ahmadi *et al*, 2010) show good results. This approach treats the particulate phase as continuous and the fluid dynamic interaction between the phases occurs through the drag coefficient.

The focus of this work is, using the framework Fluent 6.3.26, develop a fluid dynamic model of a fluidized bed in bubbling regime, with the characteristics of that found in a fast pyrolysis reactor to aftermost validation using laboratory data.

Through literature, were obtained the dimensions of a fast pyrolysis reactor bench, the characterization of the bed, drag coefficient models and CFD techniques to fluidized bed, allowing the elaboration of the computational model.

2. CHARACTERISTICS OF THE FLUIDIZED BED

According to the Geldart (1972), the particles classification is showed in Fig (1) and the sand particles are classified as belonging to group B. The characteristics of this group are:

- Formation of bubbles when the minimum fluidizing velocity is reached;
- Formation of small bubbles on distributor, that grow to cross the bed;
- Bubbles' sizes are independent of particles' size;
- Presents large recirculation.

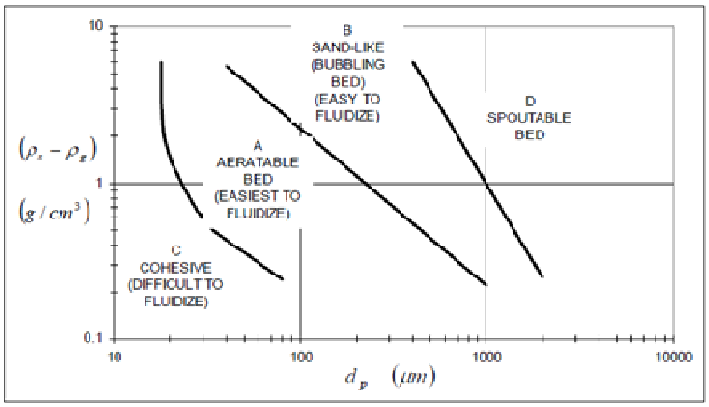

Figure 1. Geldart (1972) particles classification

Using the equations of the Geldart's work (1973), the dimensionless particle diameter (Eq. (1)) and velocity (Eq. (2)) are estimated and through Fig. (2), the flow regime in the bed is determined,

$$d_p^* = d_p \left[\frac{\rho_g(\rho_p - \rho_g)g}{\mu^2}\right]^{1/3} \tag{1}$$

$$u^* = u_o \left[\frac{\rho_g{}^2}{\mu(\rho_p - \rho_g)g}\right]^{1/3} \tag{2}$$

Where ρ_g and ρ_p are gas and solid densities respectively, g is the gravity acceleration, μ is the gas viscosity, d_p is the particle diameter and u_o is the superficial velocity.

Barbosa-Canovas and Ribas (2005) present the correlation for the porosity at minimum fluidization (Eq. (3)). Koufodimos *et al* (2008) show Reynold's number for a particle at minimum fluidization (Eq. (4)) and minimum fluidizing velocity (Eq. (5)).

$$\varepsilon_{mf} = 1 - 0{,}356(log\ d_p - 1) \tag{3}$$

$$Re_{pmf} = \frac{d_p \rho_g u_{mf}}{\mu} \tag{4}$$

$$u_{mf} = \frac{(\rho_p - \rho_g) g d_p^2}{1650\mu} \tag{5}$$

$$u_B = 0{,}3(u_o - u_{mf}) + 0{,}568\sqrt{gD_B} \tag{6}$$

$$D_B = 0{,}54(u_o - u_{mf})^{0{,}4}(h + 4\sqrt{A_o})^{0{,}8} g^{-0{,}2} \tag{7}$$

As it can be seen through the Fig. (2), Eq. (1) and Eq. (2), for the flow regime in the bubbling fluidized bed, the superficial velocity (u_o) should be between 0.36 m/s e 0.82 m/s. The minimum range value was inputted on Fluent since it is the closest to the one used by Bridgwater *et al* (2008), 0.3 m/s.

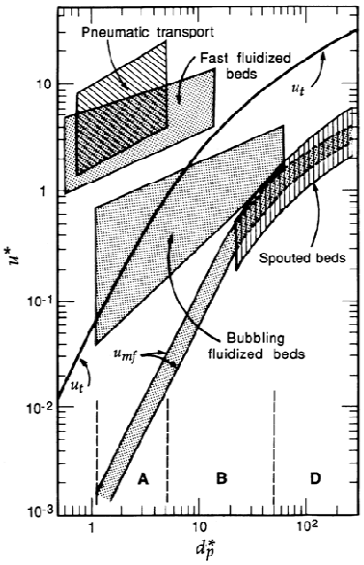

Figure 2. Flow fluidized regime classification

An important point for modeling fluid dynamics is the velocity with which the bubbles ascend in the bed (Eq. (6)) for later use in determining the simulation's time step. This information can be obtained through the correlation of Grace (1982) and the correlation for the variation of the diameter of bubbles (Eq. (7)) Van Wachem (2000), where A_o is the effective area of the distributor and h is the height of the bed. The values of u_B and D_B shown in Tab. (1) were calculated using h = 0.16 m. Since with this value D_B is greater than the diameter of the reactor, D_B was assumed to be equal to 0.04 m.

In his work, Bridgwater (2008) presents the a bench reactor dimensions, the gas characterization and the sand used, as it can be seen in Tab. (1), along with the values obtained with the equations described before.

Table 1. Physical data of the bed and the reactor

Property	Value	Comment
Superficial velocity, u_o	0.36 m/s	$\approx 2u_{mf}$
Gas density, ρ_g	1. 25 kg/m^3	Nitrogen
Gas viscosity, μ_g	1.79×10^{-5} kg/ms	Nitrogen
Solids particle density, ρ_s	2500 kg/m^3	Sand
Solids particle diameter, d_p	440 μm	Uniform distribution
Restitution coefficient, e_{ss}	0.9	Literature
Initial solids packing, ε_s	0.60	Fixed value
Static bed height h	0.08 m	Fixed value
Reactor height	0.26 m	
Reactor width	0.04 m	
Bed voidage in minimum fluidization ε_{mf}	0.41	Eq. (3)
Particle Reynolds number in minimum fluidization Re_{pmf}	4.94	Eq. (4)
Particle Reynolds number Re_p (u_o)	11	Eq. (4)
Minimum fluidization velocity u_{mf}	0.16 m/s	Eq. (5)
Maximum diameter of bubble D_B	0.04 m	Reactor width
Maximum velocity of bubble u_B	0.48 m/s	Eq. (6)

3. MATHEMATICAL MODEL

3.1. Multiphase flow governing equations

This chapter is based in Fluent 6.3 User Guide (2006).

To simulate a bubbling fluidized bed an Eulerian model will be used, where a single pressure is shared by both phases and momentum and continuity equations are solved for each phase. Accordingly, Eq. (8) is the continuity equation for phase k (k=g for gases or s for granular phases):

$$\frac{\partial}{\partial t}(\alpha_k \rho_k) + \frac{\partial}{\partial x_i}(\alpha_k \rho_k u_{ki}) = 0 \tag{8}$$

Equation (9) is the momentum equation for gas phase:

$$\frac{\partial}{\partial t}\left(\alpha_g \rho_g \overrightarrow{u_g}\right) + \nabla\left(\alpha_g \rho_g \overrightarrow{u_g}\overrightarrow{u_g}\right) = -\alpha_g \nabla P + \nabla \bar{\bar{\tau}}_g + \alpha_g \rho_g \vec{g} + K_{gs}(u_s - u_g) \tag{9}$$

Here, α_k is the volume fractions. The sum of the volume fractions of all phases is unity. The velocity vectors and density is u_k and ρ_k respectively. The pressure in the system is P.

The $\bar{\bar{\tau}}_g$ is the gas phase stress-strain tensor and it is shown in Eq. (10).

$$\bar{\bar{\tau}}_g = \alpha_g \mu_g \left(\nabla \overrightarrow{u_g} + \nabla \overrightarrow{u_g^T}\right) + \alpha_g \left(\lambda_g + \frac{2}{3}\mu_g\right) \nabla . \overrightarrow{u_g} \bar{\bar{I}} \tag{10}$$

Where λ_g is the bulk viscosity and $\bar{\bar{I}}$ is an unitary tensor.

Only the drag force is considered (K_{gs}), therefore, due the small size of the particles, the lift force is despised. The virtual mass force is also despised, since the fluid is not viscous.

Equation (11) is the momentum equation for granular phase:

$$\frac{\partial}{\partial t}(\alpha_s \rho_s \overrightarrow{u_s}) + \nabla(\alpha_s \rho_s \overrightarrow{u_s}\overrightarrow{u_s}) = -\alpha_s \nabla P + \nabla \bar{\bar{\tau}}_s + \nabla P_s + \alpha_s \rho_s \vec{g} + K_{sg}(u_s - u_g) \tag{11}$$

Where $\bar{\bar{\tau}}_s$ is the same as $\bar{\bar{\tau}}_g$. P_s is the solid pressure.

3.2. Kinetic theory of granular flow (KTGF)

The closure system of equations that describes the amount of momentum transferred within the solid phase is based on the kinetic theory of gases applied to particulate systems. Thus, this theory gets the name Kinetic Theory of Granular Flow (KTGF) and takes as premise the occurrence of instantaneous binary collisions between particles (Dan *et al*, 2010).

The macroscopic behavior of the solid phase is result of the energy from collisions and the momentum fluctuations of these particles. According to this theory, the energy associated with collisions and fluctuations is called Granular Temperature. The rheological properties and pressure of the solid phase are also functions of temperature.

3.2.1. Granular temperature

The granular temperature is a measure of the random motion of the particles. The transport equation for granular temperature can be written as Eq. (12).

$$\frac{3}{2}\left[\frac{\partial}{\partial t}(\rho_s \propto_s \Theta_s) + \nabla . (\rho_s \propto_s \vec{u}_s \Theta_s)\right] = \bar{\bar{T}}_s : \nabla \overrightarrow{us} - \nabla . q_s - \gamma_{\Theta s} - 3K_{sg}\Theta_s \tag{12}$$

3.2.2. Flux of fluctuating energy

Equation (13) describes the diffusive flux of fluctuating or granular energy,

$$q_s = k_{\Theta s} \nabla \Theta_s \tag{13}$$

where $k_{\Theta s}$ is the granular conductivity of granular temperature.

3.2.3. Collisional energy dissipation

Due to collisions between particles in the phase s, its energy is dissipated. The algebraic equation for collisional energy dissipation is showed in Eq. (14).

$$\gamma_{\Theta s} = \frac{12\,(1-e_{ss}^2)g_{0,ss}}{d_s\sqrt{\pi}}\rho_s\alpha_s^2\sqrt{\Theta_s^3} \tag{14}$$

3.2.4. Restitution coefficient

The restitution coefficient represents the ratio of particles' velocities before and after an impact, i.e. whether the impact is elastic or inelastic. The difference in velocity generates "heat", which causes increase of the granular temperature. In this work it is considered that e_{ss} = 0.9 (Bridgwater *et al*, 2010).

3.2.5. Granular viscosity

The granular viscosity (μ_s) is a summation of three viscosity contributions: the collisional ($\mu_{s,col}$), the kinetic ($\mu_{s,kin}$) and the frictional ($\mu_{s,fr}$) viscosities as in Eq. (15).

$$\mu_s = \mu_{s,col} + \mu_{s,kin} + \mu_{s,fr} \tag{15}$$

The contributions from the different viscosities vary with the flow regimes. In the dilute regime, the probability of particle collisions is low, and the mean contribution in this regime is from kinetic viscosity. In very dense particle regimes, as in regions close to the maximum packing limit, the frictional viscosity has the largest contribution. Between these two, there is the viscous regime, in which particles move like a fluid with high probability of collisions and, consequently do not reach a high velocity. Thus the collisional viscosity (Eq. (16)) has the highest contribution in the viscous regime.

As in the work of Bridgwater *et al* (2008), it was assumed the \ kinetic viscosity model developed by Gidaspow (Eq. (17)) and the frictional viscosity model of Schaeffer (Eq. (18))

$$\mu_{s,col} = \frac{4}{5}\,\propto_s \rho_s g_{0,ss}\,(1+e_{ss})\sqrt{\frac{\Theta_s}{\pi}} \tag{16}$$

$$\mu_{s,kin} = \frac{10\rho_s d_s\sqrt{\Theta_s\pi}}{96\alpha_s\,(1+e_{ss})g_{0,ss}}\left[1+\frac{4}{5}\,g_{0,ss}\propto_s\,(1+e_{ss})\right]^2 \tag{17}$$

$$\mu_{s,fr} = \frac{P_{s,fr}sin\emptyset}{2\sqrt{I_{2D}}} \tag{18}$$

where $\emptyset$ is the angle of internal friction and I_{2D} is the second invariant of the deviatoric stress tensor, which can be written as Eq. (19) and Eq. (20):

$$I_{2D} = \frac{1}{6}\,[(D_{s11}-D_{s22})^2+(D_{s22}-D_{s33})^2+\,(D_{s33}-D_{s11})^2] + D^2{}_{s12}+D^2{}_{s23}+D^2{}_{s31} \tag{19}$$

$$D_{s,ij} = \frac{1}{2}\left(\frac{\partial u_{s,i}}{\partial x_j}\right) + \left(\frac{\partial u_{s,i}}{\partial x_i}\right) \tag{20}$$

3.2.6. Frictional pressure

The frictional pressure arises when the particles are so close that they remain in contact all the time, turning\ random motion e minimal. In the frictional regime the pressure reaches a higher value than in the other regime because here the particles have very little space to move.

In this work, it was used the model due to Syamlal *et al* (1993, cited in Ahmadi *et at*, 2010) Eq. (21).

$$P_{s,fr} = 10^{25}\left(\propto_s - \propto_{min,fr}\right)^{10} \tag{21}$$

3.2.7. Granular bulk viscosity (λ_s)

The granular bulk viscosity is the resistance granular particles have to compression or expansion. The model used in this work is due to Lun *et al* (1984, cited in Bridgwater *et al*, 2008), Eq. (22).

$$\lambda_s = \frac{4}{3} \alpha_s \rho_s d_s (1 + e_{ss}) \sqrt{\frac{\Theta_s}{\pi}} \tag{22}$$

3.2.8. Solids pressure

The solids pressure, Eq. (23), represents the normal force due to particle interactions. The model used in this work is due to Lun *et al* (1984, cited in Bridgwater *et al*, 2010).

$$p_s = \alpha_s \rho_s \Theta_s + 2\rho_s(1 + e_{ss})\alpha_s^2 g_{0,ss} \Theta_s \tag{23}$$

3.2.9. Radial distribution function

The radial distribution function, Eq. (24), modifies the collisions probability between particles. The model used in this work is due to Lun *et al* (1984, cited in Bridgwater *et al*, 2010)

$$g_{0,ss} = \left[1 - \left(\frac{\alpha_s}{\alpha_{s,max}}\right)^{\frac{1}{3}}\right]^{-1} \tag{24}$$

where $\alpha_{s,\max}$ is the maximum solid volume fraction.

3.3. Drag model

Following Bridgwater *et al* (2008), the drag model used in this work was the one proposed by Gidaspow (1994).

The Gidaspow model is based on two distinct models: Wen and Yu drag model and the Ergun equation (Halvorsen and Lundberg, 2007).

Obtained from empirical data, the model of Wen and Yu (1966) is valid for dilute systems, i.e. with gas volume fraction greater than 0.8 and can be written as Eq. (25) (Gidaspow 1994)

$$K_{sg} = \frac{3\rho_g \alpha_g (1-\alpha_g)}{4 d_p} C_D |\vec{u}_s - \vec{u}_o| \, \alpha_g^{-2.65} \tag{25}$$

where C_D is the drag factor for spherical particle, obtained through Eq. (26), and $\vec{u}_s$ is the particle velocity.

$$C_D = \frac{24}{\alpha_g Re_s}\left[1 + 0.15 \left(\alpha_g \, Re_s\right)^{0.687}\right] \tag{26}$$

For gas volume fractions smaller than or equal to 0.8, the classic value used the classical Ergun equation (Halvorsen and Lundberg, 2007) is considered.

The first term of the Ergun model, as it can be seen in Eq. (27), for completely spherical particles, describes the viscous regime, which is characteristic of flow at low Reynolds number. The second term describes the kinetic regime, which is characteristic of flow at high Reynolds number.

$$K_{sg} = 150 \frac{\mu_g (1-\alpha_g)^2}{\alpha_g {d_s}^2} + 1.75 \frac{\rho_g (|\vec{u}_o - \vec{u}_s|)\,(1-\alpha_g)}{d_s} \tag{27}$$

4. COMPUTACIONAL MODEL

4.1. Geometry and mesh

From the data of the reactor used in the work of Bridgwater (2008), shown in Tab. 1, a 2D geometry was implemented, using the software ICEM 11.

In their work, Battaglia *et al* (2008) show that in the regime of bubbling bed, two-dimensional models yield comparable results to 3D models, with the advantage of reducing the computational effort significantly.

Still according to Battaglia *et al* (2008), the grid resolution must be no more than ten times the diameter of the particles. Thus, a 61X11 mesh was prepared in ICEM 11, totaling 671 square elements, since the mesh is structured.

4.2. Boundary condition

The gas velocity at the inlet was considered uniform. Non-slip conditions were imposed at the walls. At the outlet plane, a zero relative pressure, which is called in Fluent as "pressure-outlet", was considered.

4.3. Computational procedure

Using the software Fluent 6.3.26 a Intel Core2Duo 2 GHz processor based computer, the model was simulated with double precision, in transient regime and using first order discretization scheme during the first 1000 time steps in order to achieve fast convergence to an approximate solution. After this, a second order formulation was used, in order to obtain more a more accurate solution.

According to Cornelissen *et al* (2007), the time step must be determined taking into account the Courant number (N_C). For the system to be stable, the result of Eq. (28) should be less than 1 for all cells in the calculation domain. Based on the grid resolution, the bubble rise velocity and Nc = 0.01, a time step equals to 9 10^{-5} s was used.

$$N_c = v_B \frac{\Delta t}{\Delta y} \tag{28}$$

Cornelissen *et al* (2007) also report that better results are obtained for bubbling systems where a laminar flow regime is considered.. Accordingly, and for a faster convergence, it was assumed that the initial velocity of the solid phase was $\frac{u_{mf}}{\propto_{mf}}$ and the fluid phase u_{mf} (Ahmadi *et al*, 2010).

For all other sets, default values of the software were assumed.

5. RESULTS AND DISCUSSIONS

Eighty four calculation hours were needed to perform 111000 time steps, which corresponds to 10s of simulation. As convergence criterion at each time step, the residual value was monitored to be less than 10^{-3}. Two criteria were used to test convergence of the simulation. First, repetition of the volume-weighted average profile of the solid volume fraction, of the solid velocity and relative pressure, all of them measured at a plane situated 5 cm in height in the bed, over time, should be observed, as shown in Fig. (3). It is also possible to notice in Fig. (3), three separate fluid dynamic behaviors, identified by 1,2 and 3, in the time intervals between 1-4 seconds, 4-6 seconds and 6-10 seconds respectively.

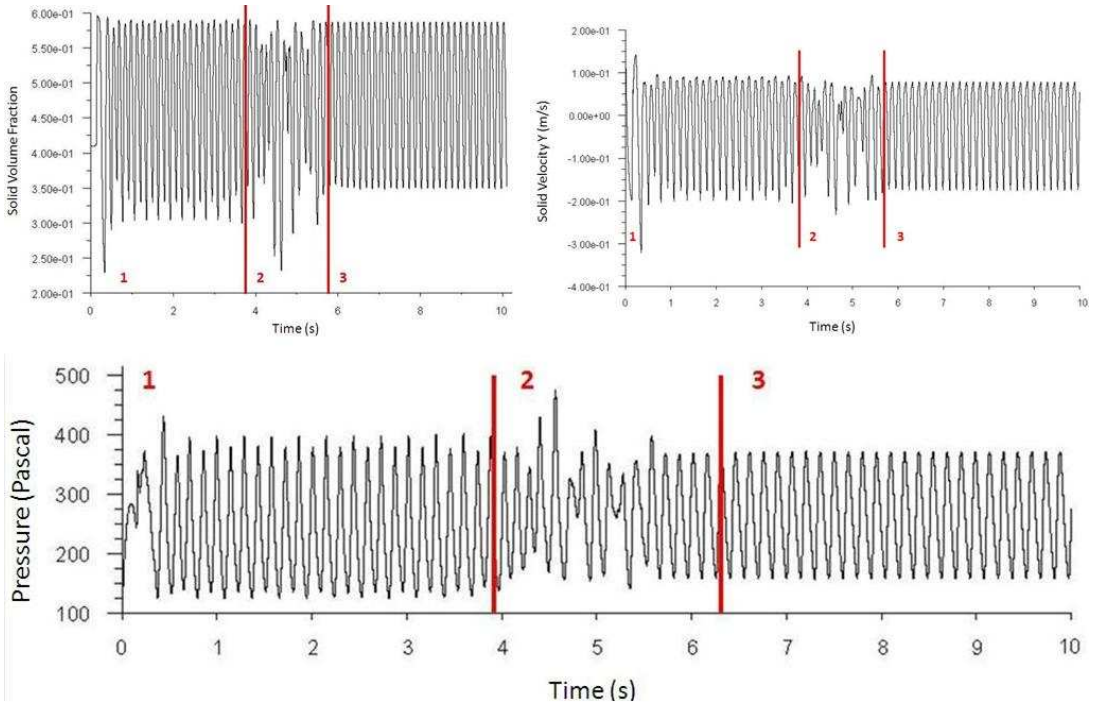

Figure 3. Evolution profiles of pressure, particle velocity and solid volume fraction

As a second criterion the similarity between the time averages of solid volume fraction obtained through a local average of solid volume fraction of eighteen points along the bed in the time intervals between 7.0 to 8.1 seconds, 7.0 to 9.1 seconds and 7.0 to 10.0 seconds were considered. It is observed in Fig. (4) that the profiles for the three intervals show a great similarity, indicating the convergence of the model.

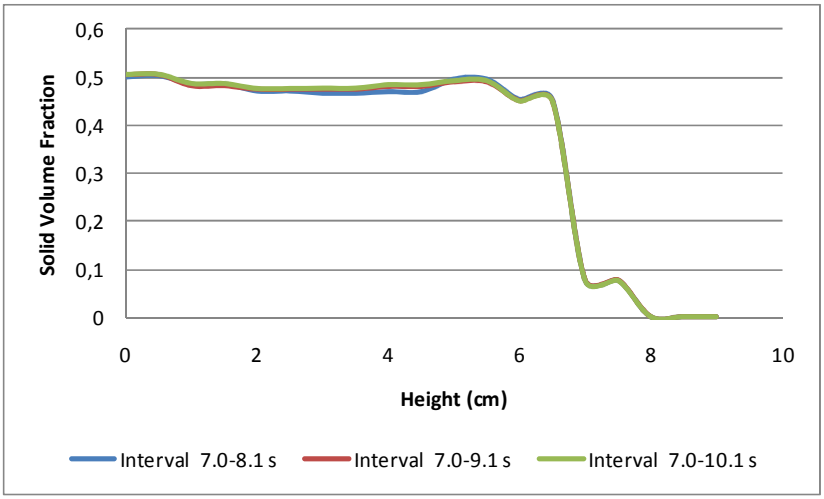

Figure 4. Time averages of solid volume fraction profiles at bed height

The calculation procedure showed a fast convergence and a good stability after approximately 0.5 seconds, as stated by Ahmadi *et al* (2010), thus indicating the adequacy in the choice of the of the solid and fluid phase initial velocities

Figure 5 shows the solid volume fraction profile for each of the three behaviors identified in Fig. (3). The profiles a, b and c correspond to the flow patterns 1, 2 and 3 respectively.

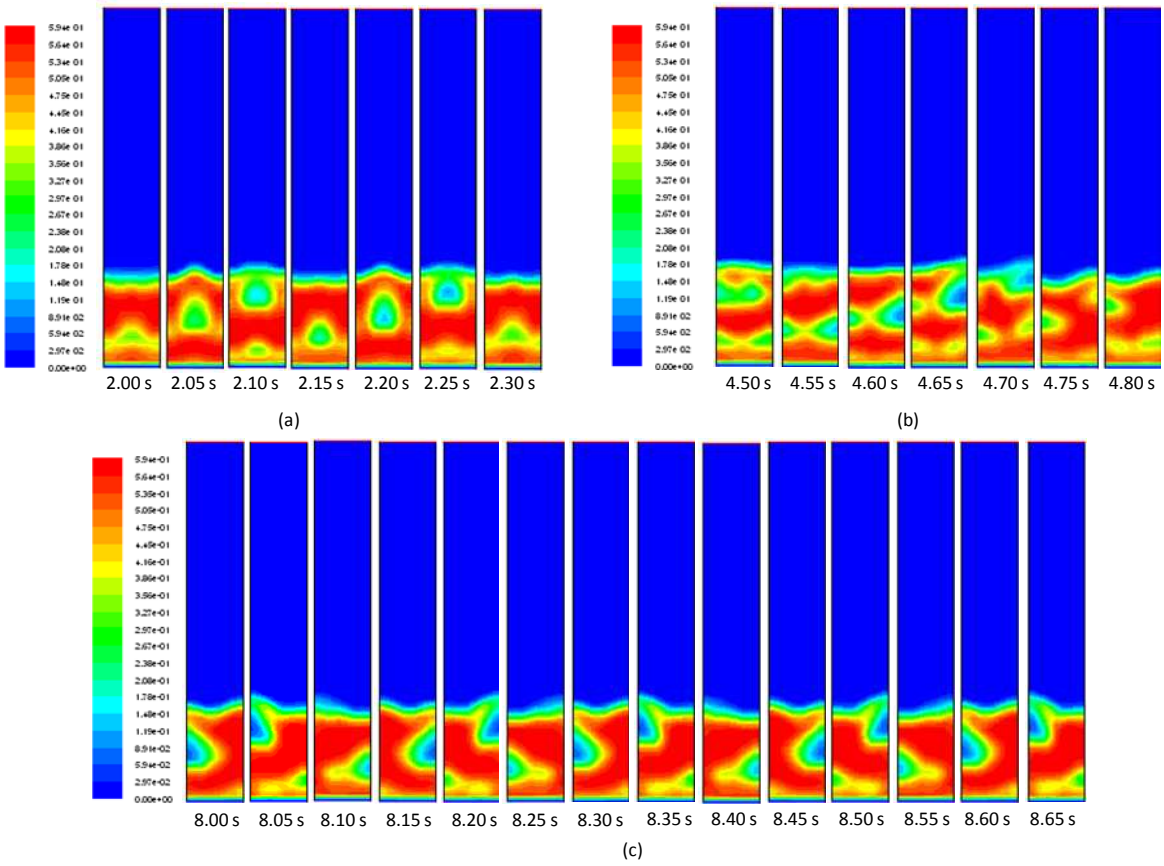

Figure 5. Solid volume fraction profiles in differents behaviors

Bridgwater (2008) presents a profile of solid volume fraction, obtained from his model in the time interval between 0 - 2.5 s, as can be seen in Fig. (6).This profile is quite similar to the profile (a) in Fig. (5).

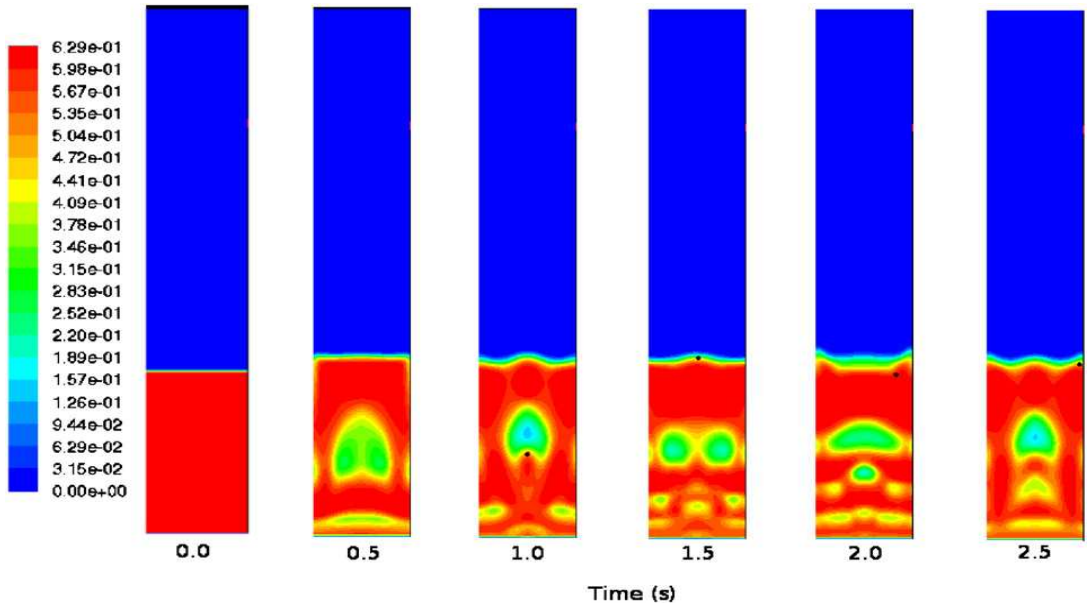

Figure 6. Bridgwater (2008) solid volume fraction profiles in 2D

Before using the model obtained in this study as a basis for simulation of a fast pyrolysis reactor, it is necessary to perform the test of mesh independence using finer meshes and to compare the results using other models of drag coefficient. In the continuation of this research, heat and mass transfer between the phases as well as the proper modelling of the reaction kinetics must be included.

6. CONCLUSION

The modelling work of fluid flow in a bubbling fluidized bed was presented. The model is part of a research work that aims the development of a fluidized bed reactor for fast pyrolysis biomass. Using a 2D geometry and Eulerian approach, integrated with the kinetic theory of granular flows, a gas-solid bed including Geldart B particles was simulated. The drag coefficient model used was one developed by Gidaspow (1994). The model was implemented numerically by means of the Fluent 6.3.23 platform.

The model showed a rapid convergence and good stability, checked by repetition of the profile of the volume-weighted average of solid volume fraction, of the solid velocity and relative pressure, beyond the temporal average over the height of the bed.

From the observation of the profile of solid volume fraction, it is possible to notice three distinct behaviors over time. Comparison of the results obtained in the time interval between 2.00 and 2.30 seconds shows that these agree well with the result obtained by Bridgwater (2008), which indicates the suitability of the model obtained in this work for use as a basis for future works.

In the continuation of the research work using the model obtained herein, it will be necessary to perform the mesh independence test, using more refined meshes and comparing the results obtained using other models for the drag coefficient. Besides that, heat and mass transfer between the phases as well as the proper modelling of the reaction kinetics must be included.

7. REFERENCES

Ahmadi, G., Hosseini, S.H., Nasr, M., Rahimi, R. and Zivdar, M.,2010, “CFD studies of solids hold-up distribution and circulation patterns in gas–solid fluidized beds”, Powder Technology, Vol.200, pp. 202-215.

Apte, S.V., Lundgren, T., and Mahesh, K.,2003, “A Eulerian Lagrangian model to simulate two-phase/particulate flows”, Centre for Turbulence Research, Annual Research Briefs, pp. 161-171.

Barbosa-Cánovas, G.V. and Ribas, A.I.,2005, “Operaciones Unitarias en la Ingeniería de Alimentos - Tecnología de Alimentos”, Ed. Mundi-Prensa Libros, Madrid, Spain, 825 p..

Battaglia, F., Pannala, S. and Xie, N.,2008, “Effects Of Using Two- Versus Three-Dimensional Computational Modeling Of Fluidized Beds Part I, Hydrodynamics”, Powder Technology, Vol.182, pp. 1-13.

Bridgwater, A.V., Gu, S. and Papadikis, K.,2008, "CFD modelling of the fast pyrolysis of biomass in fluidised bed reactors, PartA: Eulerian computation of momentum transport in bubbling fluidised beds", Chemical Engineering Science, Vol.63, pp. 4218-4227.

Bridgwater, A.V., Gu, S. and Papadikis, K.,2010, "Computational modelling of the impact of particle size to the heat transfer coefficient between biomass particles and a fluidised bed", Fuel Processing Technology, Vol.91, pp. 68-79.

Bridgwater, A.V., Meier, D. and Radlein, D.,1999, "An overview of fast pyrolysis of biomass", Organic Geochemistry, Vol.30, pp. 1479-1493.

Bridgwater, A.V. and Peacocke, G.V.C.,2000, "Fast pyrolysis processes for biomass", Renewable and Sustainable Energy Reviews, Vol.4, pp. 1-73.

Cornelissen, J.T., Ellis, N., Escudié, R., Grace, J.R. and Taghipour, F.,2007, "Cfd Modelling Of A Liquid–Solid Fluidized Bed", Chemical Engineering Science, Vol.62, pp. 6334-6348.

Dan,S., Gidaspow, D., Huilin, L., Jianzhi, W., Juhui, C., Ming, C., Yunhua, Z., 2010, "Numerical simulation of gas-particle flow with a second-order moment method in bubbling fluidized beds", Powder Technology, Vol.199, pp. 213-225.

Depypere, F., Dewettinck, K. and Pieters, J.G.,2004, "CFD analysis of air distribution in fluidised bed equipment", Powder Technology, Vol.145, pp. 176-189.

Fluent Inc.,2006, "FLUENT 6.3 User's Guide", 2006.

Geldart, D.,1972, "The Effect of Particle Size and Size Distribution on The Behaviour of Gas-Fluidized Beds", Powder Technology, Vol.6, pp. 201-215.

Geldart, D.,1973, "Types of Gas Fluidization", Powder Technology, Vol.7, pp. 258-292.

Grace, J. R.,1982, "Fluidized-Bed Hydrodynamics" In Hetsroni, G.,2006, Handbook of Multiphase Systems, ed. Hemisphere, Washington D.C., EUA, 1156 p..

Gidaspow. D.,1994, "Multiphase Flow and Fluidization-Continuum and Kinetic Theory Descriptions", Ed. Academic Press, San Diego, CA, USA, 467 p..

Halvorsen, B.M. and Lundberg, J.,2007, "A Review Of Some Exsisting Drag Models Describing The Interaction Between Phases In A Bubbling Fluidized Bed", Telemark Technological R&D Centre, pp. 1-8.

Hamzehei, M., and Rahimzadeh, H.,2009, "Experimental and numerical study of hydrodynamicswith heat transfer in a gas–solid fluidized-bed reactor at different particle sizes", Industrial & Engineering Chemistry Research, Vol.48, pp. 3177-3186.

Koufodimos, G., Samaras, Z., Skoulou, S. and Zabaniotou, A.,2008, "Conceptual Design and Preliminary Hydrodynamic Study of an Agro Biomass Bench Gasification Fluidized Bed Reactor", Reactor Engineering, Vol.6, pp. 1-17.

Van Wachem, B.G.M., 2000, "Derivation, Implementation and Validation of Computer Simulation Models for Gas-Solid Fluidized Beds", PhD Thesis, TU Delft, Netherlands, 198 p..

8. RESPONSIBILITY NOTICE

The authors are the only responsible for the printed material included in this paper.